Chapter 3

Buckling Instability in Physical LC Gels

The work described in this chapter was a collaborative effort with Professor Robert B. Meyer and his graduate student Guangnan Meng at Brandeis University. We also acknowledge helpful discussions with Professor Mark Warner (Cavendish Laboratory, Cambridge University).

3.1 Abstract

We observe in a nematic gel a low-energy buckling deformation arising from soft and semi-soft elastic modes. The self-assembled gel is prepared by dissolving a triblock copolymer having a side-group liquid crystalline midblock and polystyrene endblocks in a nematic liquid crystal. Under polarized optical microscopy we observe a striped texture that forms when gels uniformly aligned at 35 ^{o}C are cooled to room temperature. We model the instability using the molecular theory of nematic rubber elasticity, and the theory correctly captures the change in pitch length with sample thickness and polymer concentration. This buckling instability adds to the library of fascinating texture transitions observed in liquid crystalline elastomers and gels.

3.2 Introduction

Rubbers, or elastomers, are unique in their ability to undergo large shape changes under external forces and then snap back to their initial shape when the forces are removed [1]. Elastomers are comprised of long, rubbery polymer strands connected together by covalent or physical bonds. These strands are initially randomly coiled, but they can stretch and change their configuration to accommodate large shape changes. In a liquid crystal (LC) elastomer, the network strands are LC polymers, and they have an anisotropic conformation that is temperature dependent and also affected by external electric and magnetic fields. Similarly, an LC gel is composed of an anisotropic polymer network swollen with solvent. Unlike conventional elastomers or gels, LC elastomers and gels are predicted to undergo "soft" and "semi-soft" deformations in which they can change shape at little cost to the free energy [2, 3, 4, 5]. These low-energy deformations are enabled by the anisotropy in the polymer network strands; when a strain is imposed on an LC elastomer, the network strands can accommodate the strain by rotating their sense of anisotropy instead of deforming the end-to-end distance of the chains, which is energetically more costly. Soft deformations oftentimes give rise to periodic textures [6], and they can also result in significant shape changes to temperature [2] or other external influences such as UV light [7, 8, 9].

Recently, we produced an LC gel by the physical association of a copolymer comprised of a side-group LC polymer (SGLCP) midblock and polystyrene (PS) endblocks [10, 11] (Fig. 3.1). When the LC gel is uniformly aligned and confined between rigid plates, it exhibits a reversible, striped texture change with small changes in temperature. Similar striped textures have been observed in LC elastomers[6, 4], but the instability observed here is unique for its geometry and sensitivity to small changes in temperature. We present the details of the striped texture in the physical gels, and we formulate a description of the instability based on the molecular theory of nematic rubber elasticity. The theory accounts for the changing network anisotropy, which in an unconfined sample would cause the gel to change shape macroscopically. Instead, due to the confining substrates which impose a no-slip condition, the gel undergoes a semi-soft deformation that involves a periodic modulation of the nematic director; in other words, the gel "buckles." The theory correctly accounts

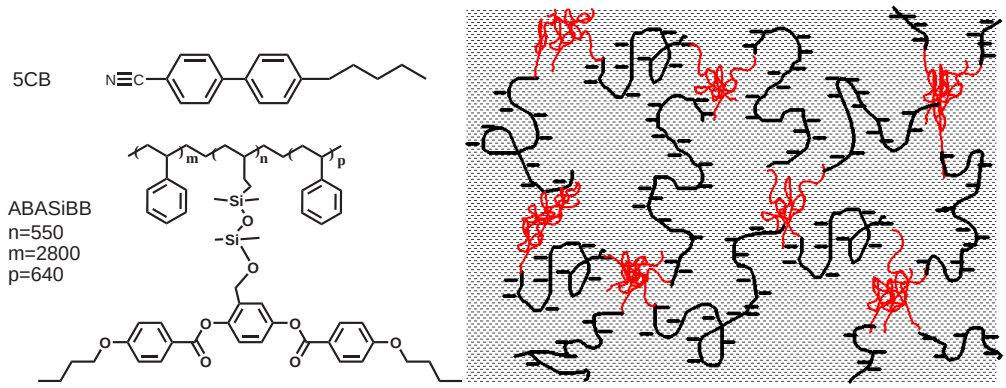

Figure 3.1: (a) Chemical structure of LC 5CB and the end-associating triblock copolymer used in this study, and (b) a schematic of the LC gel. The midblock is a random copolymer of LC side-group and butadiene monomer, with the LC side-group composing approximately 70 mol % of the midblock. The polydispersity ($\frac{M_w}{M_n}$) of the triblock is approximately 1.6, as measured by gel-permeation chromatography. In the schematic, the speckled background represents the LC solvent 5CB, the dark black lines represent the SGLCP midblock, and the red chains represent the polystyrene endblocks.

for the observed dependence of the stripe texture pitch and threshold temperature on the sample thickness and polymer concentration.

3.3 Experimental

The triblock copolymer was prepared by polymer-analogous synthesis starting with a polystyrene – *block* – 1,2-polybutadiene – *block* – polystyrene triblock copolymer, as described in Chapter 2. The self-assembled gels are prepared by dissolving the resulting high molecular weight ($\sim$ 1500 kg/mol) PS - SGLCP - PS triblock copolymer in the nematic LC 4-cyano-4′-n-pentylbiphenyl (5CB) (Fig. 3.1) [10]. The polystyrene block is considerably less soluble than the SGLCP block in 5CB, and in the nematic phase of 5CB the endblocks form aggregates which physically crosslink the triblock polymers. The resulting self-assembled network has a uniform molecular weight between crosslinks defined by the size of the SGLCP midblock.

In this work, we study gels with polymer concentrations of 10 wt % or less. Samples were loaded into cells with well-defined gap spacings and alignment layers. For gaps smaller than 10 μm, we used cells purchased from LC Vision. The cells consist of indium-tin-oxide coated glass plates with a layer of SiO_2 to induce planar alignment. For gaps larger than 10 μm, we used glass slides with

teflon spacers and a rubbed polyimide layer for alignment. The cell thickness was determined with a UV/vis spectrophotometer by interferometry for gaps smaller than 10 μm [12] or by measuring the thickness with a micrometer for larger gaps. The nematic gels thermoreversibly transition to a viscous liquid when heated above the nematic-isotropic phase transition temperature (T_{NI}) of 5CB, 35.2 ^{o}C, and this allows for easy loading of the gel into the cell gap.

A magnetic field or shear was used to form uniform nematic monodomains. In the first case, the gel was placed in an 8.8 T magnetic field oriented parallel to the desired director orientation, heated above its T_{NI}, and allowed to cool to room temperature. After removing the cell from the magnetic field, the cell was heated to 34 ^{o}C and then cooled back down to room temperature at 1 ^{o}C/min to remove any residual irregularities. In some cases it was easier to use shear to align the sample. Shear proved effective in eliminating bubbles and defects at the solid-gel interface that were difficult to eliminate using magnetic field alignment. In order to shear align the sample, the sample was loaded into a Mettler FP 82 hot stage and the temperature set to 34.5 ^{o}C while the top slide was carefully moved back and forth across the sample.

3.4 Results

3.4.1 Details of the stripe texture

Gels that are uniform monodomains at 35 ^{o}C develop a striped texture visible under polarized optical microscopy when cooled to room temperature (Fig. 3.2). The periodic texture reversibly disappears and reappears when the gel is heated above and then cooled below a threshold temperature for stripe formation, and the pitch length of the striped texture is independent of temperature. The stripes run perpendicular to the initial director orientation $\underline{n}_o$. Rotating the crossed polarizer/analyzer pair by approximately $\pm 15^o$ relative to $\underline{n}_o$ maximizes the contrast between dark and bright bands, and the regions in the sample that appear dark at $+15^o$ appear bright at -15^o and vice-versa (Fig. 3.2). The stripes are less evident but still visible when the polarizers are aligned with $\underline{n}_o$. These observations indicate that the director rotates within the plane and in opposite directions in adjacent stripes but

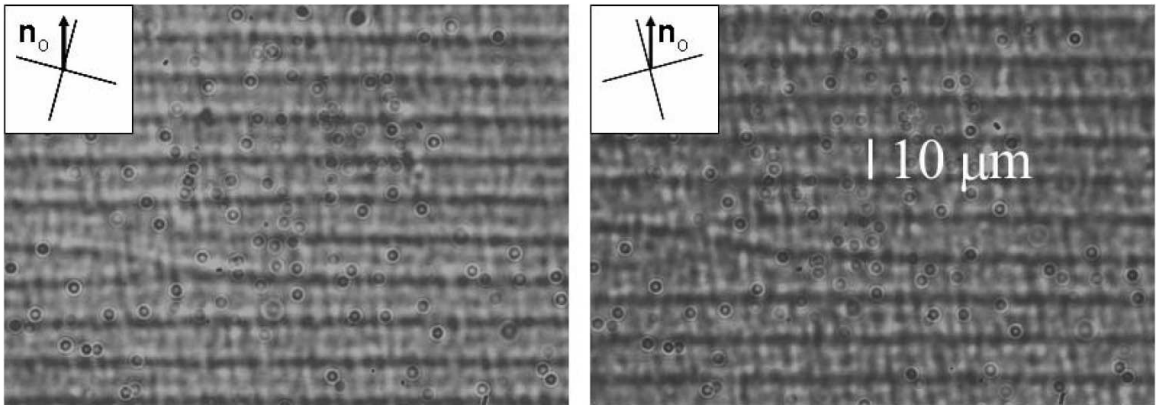

Figure 3.2: A 5 wt % gel in a 25 μm gap at 20.0 ^{o}C viewed with a polarizing optical microscope. The orientation of the director imprinted during crosslinking n_o and the orientation of the crossed polarizers is shown in the top left-hand corner of each image. Note that the dark lines, which represent regions in which the director is locally aligned with an axis of the crossed polarizers, shift positions in the left- and right-hand images, which were taken for the same sample in the same position and orientation but with a different orientation of the crossed polarizers. The positions of the extinction bands in the images are shifted relative to each other, and this indicates a spatially varying director orientation in the sample. The scale bar in the image shows the pitch length of approximately 10 μm for this particular sample.

does not preclude an out-of-plane rotation of the director coupled with this in-plane rotation.

The characteristics of the striped texture depend on the sample thickness and polymer concentration. The pitch length is larger in thicker samples and more dilute gels (Fig. 3.3). Stripes do not appear when the gap is too thin or the polymer concentration too dilute. In the case of a 5 wt % gel, stripes do not appear in 4- and 9-μm-thick cells but they do appear at larger gap thicknesses. For 10 wt % gels, stripes appear in the thinnest gaps tested, 4 μm.

3.4.2 Mathematical model

We propose that the buckling instability arises from a combination of rubber elasticity and LC elasticity, and that the instability represents a periodic network strain coupled to a periodic rotation of the director. We can formulate a molecular model of the instability by utilizing the theory for nematic rubber elasticity developed for LC elastomers [2, 13]. This theory assumes that the network is composed of anisotropic, gaussian chains and neglects excluded volume interactions. The anisotropic conformation of the polymer strands can be described by a step-length tensor $l_{ij} = l_\perp \delta_{ij} + (l_\parallel - l_\perp) n_i n_j$, where $l_\perp$ and $l_\parallel$ are the step lengths perependicular and parallel, respectively,

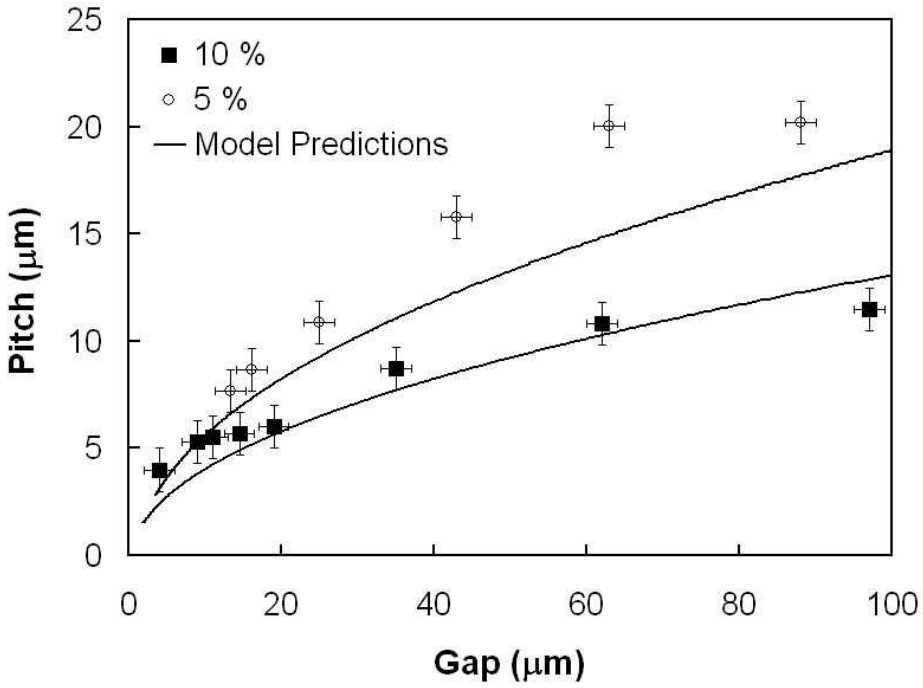

Figure 3.3: Dependence of pitch on gap in 10 and 5 wt % polymer gels.

to the nematic director for a freely jointed chain. These step lengths are directly related to the mean square end-to-end distance, $\langle R_i R_j \rangle = \frac{1}{3} l_{ij} L$, where L is the arc length of the polymer chain. A more useful expression relates the ratio of the step lengths to the ratio of the radii of gyration of the chain, $\frac{l_\parallel}{l_\perp} = (\frac{R_\parallel}{R_\perp})^2$. For the present polymer, which has a strongly prolate conformation (see Chapter 5, Fig 5.1), r is greater than 1 and decreases towards 1 as the temperature increases towards the T_{NI}. The ratio of the step lengths $\frac{l_\parallel}{l_\perp}$ is denoted as the network anisotropy r, and the anisotropy during crosslinking is denoted as r_o.

The free energy density of the gel consists of three terms: ideal nematic network elasticity, non-ideal nematic network elasticity, and Frank elasticity (Eq. 3.1). The free energy cost of deforming the gel includes the contribution of the network strands, expressed in terms of the deformation gradient tensor λ_{ij} (see Chapter 1). The ideal nematic elastic term is weighted by the rubber modulus μ. The non-ideal, or semi-soft, contribution is weighted by μ and the semi-softness parameter α. Semisoft elasticity arises from imperfections in the nematic network such as compositional fluctuations [4]. The last term is the Frank elastic term, which is a penalty for non-uniform director fields. We make

the one-constant approximation [14] with Frank elastic constant K.

$$\begin{aligned} F &= \frac{1}{2}\mu\left(Tr[\underline{\underline{l_o}}\cdot\underline{\underline{\lambda}}^T\cdot\underline{\underline{l}}^{-1}\cdot\underline{\underline{\lambda}}]\right)+ \\ &\quad \frac{1}{2}\mu\alpha\left(Tr[(\underline{\underline{\delta}}-\underline{n_o}\,\underline{n_o})\cdot\underline{\underline{\lambda}}^T\cdot\underline{n}\,\underline{n}\cdot\underline{\underline{\lambda}}]\right)+ \\ &\quad \frac{1}{2}K\left((\nabla\cdot\underline{n})^2+(\underline{n}\cdot\nabla\times\underline{n})^2+(\underline{n}\times\nabla\times\underline{n})^2\right) \end{aligned} \tag{3.1}$$

In order to model the phenomena, we start with a macroscopically uniform nematic gel in which the director $\underline{n}$ is aligned in a unique direction parallel to the substrates of the cell. Below a critical temperature, r becomes sufficiently large that the gel buckles. We assume that the director stays in the $x-y$ plane and that the director orientation depends on x and z but is independent of y. (Fig. 3.4). Coupled to the director rotation is a network strain field described by the deformation gradient tensor λ_{ij}. At the interface with the cell ($z=\pm\frac{d}{2}$), the substrates impose the boundary conditions of no-slip. We analyze the behavior near the transition to the striped state, where we assume small values for the amplitudes of the director rotation and the displacements. The displacement field $\underline{\Delta}$ satisfies the conditions of no-slip at the substrates ($\underline{\Delta}=0$ at $z=\pm\frac{d}{2}$) and incompressibility ($\nabla\cdot\underline{\Delta}=0$). Also, the displacement field and director rotation are independent of y.

We can develop simple sinusoidal functions (Eq. 3.2) that satisfy the boundary conditions, as follows. First, we assume a simple sinusoidal dependence for the director orientation, $\phi\sim\cos kx$,

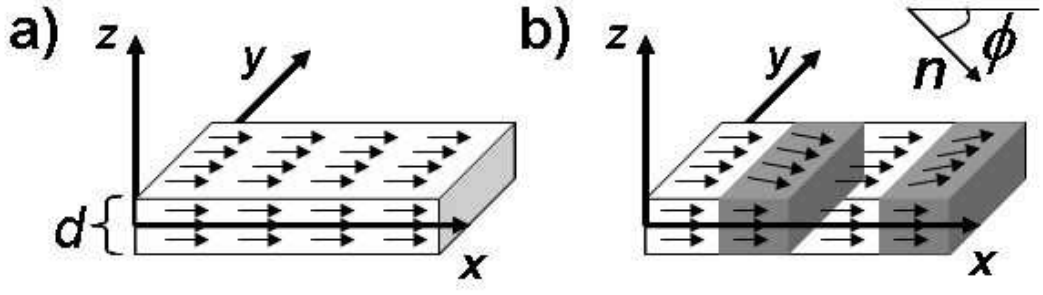

Figure 3.4: Nematic gel director orientation in **a)** the initial uniformly aligned state, and **b)** the striped state. The cell substrates are at $z=\pm\frac{d}{2}$.

where k is a constant that sets the wavevector for the distortion. Note that the pitch length in Fig. 3.2 corresponds to half the pitch of this periodic function, $\frac{\pi}{k}$. Since the director is confined to the $x-y$ plane, $\Delta_z = 0$ everywhere. It then follows, from the condition of incompressibility, that Δ_x is independent of x, and therefore Δ_x must also zero everywhere to be compatible with the symmetry of the nematic phase. Therefore, Δ_y is the only non-zero component of the displacement field $\underline{\Delta}$. The y displacement will be out of phase with the director rotation (the deformation gradient is in phase with the rotation), giving $\Delta_y \sim \sin kx$.

Since the director is coupled to the undeformed network at the substrates it retains the same orientation present during crosslinking. Director rotations independent of network deformations are in general costly, with $F \sim \frac{1}{2}\mu\phi^2$ for such rotations [2]. Therefore, $\phi = 0$ at $z = \pm\frac{d}{2}$. We also assume a simple sinusoidal dependence $\cos qz$, with $q = \frac{\pi}{d}$, for the director rotation and network strain fields along the z-axes. Note that this function decays to zero at the substrate interface. Finally, the terms ξ and γ set the amplitudes of the rotation and displacement fields, respectively (Eq. 3.2).

$$\begin{aligned} \phi(x,z) &= \xi\cos(qz)\cos(kx), \\ \Delta_y &= \gamma\cos(qz)\sin(kx), \\ \Delta_x &= \Delta_z = 0 \end{aligned} \tag{3.2}$$

We can calculate the deformation gradient tensor $\underline{\underline{\lambda}}$ from the displacement field ($\lambda_{ij} = \delta_{ij} + \frac{\partial\Delta_i}{\partial x_j}$), and substitution of $\underline{\underline{\lambda}}$ and $\underline{n}$ into Eq. 3.1 gives the free energy density of an incompressible nematic gel subject to the periodic deformation and director rotation described by Eq. 3.2. We Taylor expand this function in ξ around $\xi = 0$ and keep only terms of $\mathrm{O}(\xi^2)$ or greater. Next, we integrate the simplified free energy density over one wavelength of the deformation to obtain the average free energy density of the gel. Subtracting the energy of the uniformly aligned gel from this free energy gives the free energy relative to the monodomain state, so that a crossing from a positive to a negative value in the free energy indicates an onset of the buckling instability. (Eq. 3.3).

$$
\begin{aligned}
F = \quad & \frac{1}{8}K\xi^2(k^2+q^2) + \\
& \mu\{\frac{1}{8}\gamma^2(q^2+k^2r_o) + \frac{r_o}{4}\gamma\xi k(\frac{1}{r}-1) + \\
& \frac{1}{8}\xi^2(r_o-1+\alpha+\frac{1}{r}-\frac{r_o}{r})\}
\end{aligned}
\tag{3.3}
$$

The first term in (Eq. 3.3) is the contribution from Frank elasticity and is always positive, as expected. The second, bracketed term (weighted by μ) is the contribution from nematic rubber elasticity, and it contains some terms that contribute negative values to the free energy. The various terms in the bracketed expression are grouped according to whether they arise from ideal or non-ideal nematic rubber elasticity. The first two terms in the bracketed expression, $\frac{1}{8}\gamma^2(q^2+k^2r_o)$ and $\frac{r_o}{4}\gamma\xi k(\frac{1}{r}-1)$, are the ideal or soft rubber elastic terms. The term $\frac{r_o}{4}\gamma\xi k(\frac{1}{r}-1)$ is always negative for $\gamma\xi > 0$ and is resposible for the buckling instability, while the term $\frac{1}{8}\gamma^2(q^2+k^2r_o)$ is always positive and increases the threshold to the buckled state.

The final term in the bracketed expression, $\frac{1}{8}\xi^2(r_o-1+\alpha+\frac{1}{r}-\frac{r_o}{r})$, is the contribution from non-ideal network elasticity. This term is always positive, and it arises from two sources of semi-softness, or non-ideality. The first source, weighted by α, accounts for compositional fluctuations or polydispersity in the molecular structure. α is always positive or zero, and a greater value of α indicates a greater degree of semi-softness. The second source of semi-softness arises from the anisotropy during crosslinking r_0. A perfectly soft network has $r_0 = 1$ and a perfect memory of the isotropic state [2]. Note that if $\alpha = 0$ and $r_0 = 1$, the semi-soft contribution vanishes.

In order to compute an anisotropy and wavevector for this general case, we look for the minimum value of r and critical wave vector k for which the right combination of infinitesimal displacement γ and rotation ξ costs zero energy (Eq. 3.4), signalling an instability as r passes through this value. For slightly larger r values, the amplitude of the instability grows rapidly, with the wavelength determined at the instability.

$$\gamma = \frac{kr_0\xi(r-1)}{r(q^2+k^2r_0)} \tag{3.4}$$

The material parameters can be reasonably approximated from independent measurements or from known properties of the liquid crystal solvent 5CB. For example, the LC elastic constants K have been measured previously for 5CB at room temperature [12, 15] and have values of about 1×10^{-11} N. We measured the rubber modulus μ in a cone-and-plate rheometer and obtained a value of approximately 220 Pa for a 10 wt % gel and 50 Pa for a 5 wt % gel [10]. The endblocks associate at a temperature near the T_{NI} to form the gel, so we set the initial anisotropy r_o to the small value of 1.2. In addition to these parameters, we reasonably approximate the semi-softness parameter α to have a value of 0.05, based on previous studies of nematic elastomers [16].

3.5 Discussion

A periodic modulation of the nematic director is unexpected because it introduces a free energy contribution from Frank elasticity. The appearance of the stripes can be accounted for, however, by including the rubber elastic energy of the polymer network. (A periodic striped texture has also been observed in very thin (< 1 μm) films of small molecule nematic LC due to surface gradient terms in the elastic free energy expression [17, 18]. Our samples are thick enough that the surface gradient terms are not significant.) An SGLCP dissolved in a nematic solvent adopts an anisotropic chain conformation coupled to the nematic order of the solvent [10]. Based on prior literature on nematic elastomers [2], we expect that an unconstrained free standing gel will change shape: in the case of a strongly prolate alignment tendency, the gel will expand in the direction of director orientation with decreased temperature (our gel is too soft to carry out the same experiment). When constrained between glass plates, however, expansion of the gel in the direction of increasing anisotropy is prevented by the boundary conditions, and the network becomes increasingly frustrated as the temperature decreases. Increasing network elastic energy results in a buckling instability in which a periodic strain field reduces the rubber elastic free energy at the cost of a Frank elastic penalty.

Such a spontaneous deformation is possible only in nematic rubbers, where a coupling between the local nematic director orientation and macromolecular conformation significantly reduces the rubber elastic penalty associated with mechanical deformations, a phenomenon known as soft elasticty [2]. This coupling gives rise to macroscopic shape changes in nematic rubbers in response to heat and light and director rotations in response to strains.

It is instructive to look at the behavior predicted by Eq. 3.3 for various limiting cases. First, an infinitely small spatial frequency $k \approx 0$, or equivalently an infinitely large pitch, results in a positive free energy relative to the unbuckled state. This can be easily seen in Eq. 3.3 by noting that the only negative term in the expression, $\frac{r_o}{4}\gamma\xi k(\frac{1}{r}-1)$, disappears when $k = 0$. This indicates that there is always energetic penalty, from both LC elasticity and nematic rubber elasticity, for buckling in a sample of finite thickness. The penalty arises from the boundary condition which necessitates a bend distortion and shearing from the edges to the center of the sample.

In the case of an infinitely thick sample, $q \approx 0$, the penalties $\frac{1}{8}K\xi^2q^2$ and $\frac{1}{8}\gamma^2q^2$ for the bend distortion and shearing, respectively, vanish. If the gel is perfectly soft ($\alpha = 0$ and $r_0 = 1$), then the buckling instability carries no penalty from the rubber elastic term. This can be seen in the free energy expression (Eq. 3.3): In the limit $q \to 0$, the negative contribution $\sim r_o\gamma\xi k(\frac{1}{r}-1)$ can always compensate the positive contributions for any k by properly selecting γ and ξ. For $r > 1$, the buckling instability will always be favored over the monodomain state for a soft gel of infinite thickness. In the case of semi-soft ($\alpha > 0$ and/or $r_0 > 1$) gels in thick gaps, there is a finite threshold in r to the buckling instability.

The various contributions to the free energy are depicted graphically for a gel of finite thickness in Fig. 3.5a. The rubber elastic terms favor a large frequency. However, Frank elasticity goes inversely with the square of the wavelength, making very short wavelengths costly in energy. The final wavelength is a compromise of nematic rubber elasticity and Frank elasticity. The final wavelength is set by the rubber modulus μ, the Frank elastic constant K, the initial anisotropy r_0, and the semi-softness parameter α.

A comparison of the model prediction of the pitch and experimental results shows good qualitative

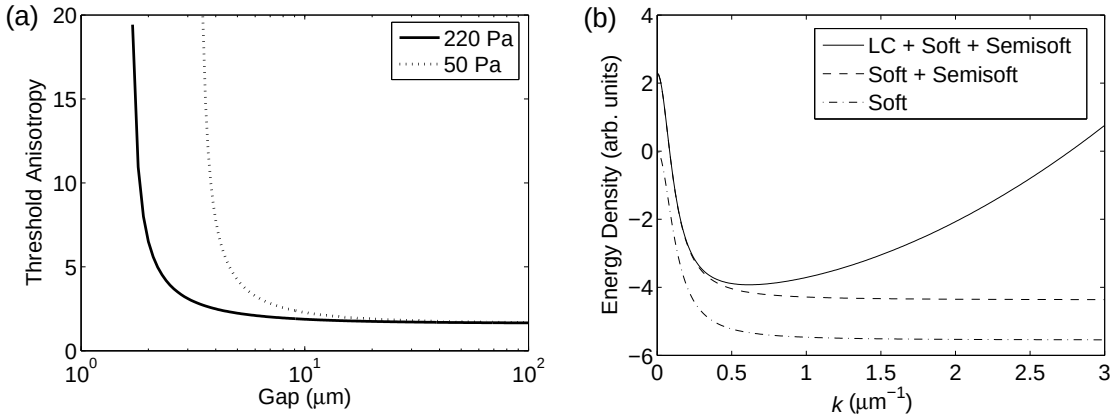

Figure 3.5: (a) Predicted value of the threshold anisotropy r_{th}, as a function of gap thickness d and rubber modulus μ. Bands form if the polymer has $r > r_{th}$. The values of μ correspond to those of the 5 wt % and 10 wt % gels. (b) The different components of the free energy expression (Eq. 3.3) for a gel with a modulus of 220 Pa, an initial anisotropy of 1.2, a present anisotropy of 3, a semi-softness parameter of 0.05, an LC elastic constant of 1×10^{-11} N, and a gap of 25 μm. The soft and semi-soft elastic parts refer to the ideal and non-ideal network elastic terms, respectively, and adding the LC part gives the full free energy density. The mimumum in the full free energy density corresponds to the predicted k for these sample conditions.

agreement (Fig. 3.3a). The model predicts the trends of increasing pitch with increasing gap and decreasing polymer concentration. The model also accounts for the disappearance of stripes at small gaps from a prediction of the threshold anisotropy (Fig. 3.5). Small-angle neutron scattering measurements show the anisotropy of the present midblock at 25^{o}C to be approximately 10 (see Fig. 5.2, Chapter 5. Based on this value, the model predicts that bands are suppressed for $d < 3.7$ μm for the 5 wt % gel and for $d < 1.9$ μm for the 10 wt % gel. As the gap decreases, q increases, increasing the cost of both Frank elasticity and nematic rubber elasticity (Eq. 3.3).

$$k = \sqrt{q\sqrt{\frac{\mu}{K}}\left(\frac{r-1}{r}\right) - \frac{q^2}{r_0}} \tag{3.5}$$

The functional dependence of the optimal wavevector on the gap has a square root dependence at large gaps (small q) (Eq. 3.5). At small enough gaps, however, for $q \sim \sqrt{\mu/K}$, the negative term in (Eq. 3.5) becomes comparable to the positive contribution. This would result in an increasing k with increasing q (longer pitch at smaller gap); however, this never occurs because the upper bound on q is $\sqrt{\mu/K}$.

To summarize, we have presented a stripe distortion that arises in uniformly aligned nematic gels in response to small temperature changes. A model based on the molecular theory of nematic rubber elasticity accounts for the observed experimental features: the onset of the instability with changes in the network anisotropy, the increase in the pitch with increasing sample thickness, the decrease in the pitch with increasing polymer concentration, and the disappearance of the instability at small sample thicknesses. The model indicates that the instability arises from a balance of Frank elasticity and polymer elasticity, resulting in a periodic structure on the length scale of micrometers.

The buckling instability in nematic gels is a remarkable transition that adds to the library of texture transitions observed in LC elastomers and gels. LC elastomers can show similarly striped states in response to mechanical strains [6, 19], and LC gels demonstrate non-uniform responses to external electric fields [20, 16]. These periodic textures in LC materials find analogy in an instability observed in deformable elastic crystals [21], which can develop an undulating texture at their surface in response to strains.

Bibliography

[1] P. J. Flory. *Principles of Polymer Chemistry.* Cornell University Press, Ithica, 1953.

[2] M. Warner and E. M. Terentjev. *Liquid Crystal Elastomers.* Oxford University Press, Oxford, 2003.

[3] M. Warner, P Bladon, and E. M. Terentjev. Soft elasticity – deformation without resistance in liquid-crystal elastomers. *J. Phys. II*, 4(1):93–102, 1994.

[4] H. Finkelmann, I. Kundler, E. M. Terentjev, and M. Warner. Critical stripe-domain instability of nematic elastomers. *J. Phys. II*, 7(8):1059–1069, 1997.

[5] E. M. Terentjev and M. Warner. Linear hydrodynamics and viscoelasticity of nematic elastomers. *Eur. Phys. J. E*, 4:343–353, 2001.

[6] I. Kundler and H. Finkelmann. Strain-induced director reorientation in nematic liquid single crystal elastomers. *Macromol. Rapid Commun.*, 16:679–686, 1995.

[7] H. Finkelmann, E. Nishikawa, G. G. Pereira, and M. Warner. A new opto-mechanical effect in solids. *Phys. Rev. Lett.*, 87(1):015501, 2001.

[8] M. Camacho-Lopez, H. Finkelmann, P. Palffy-Muhoray, and M. Shelley. Fast liquid-crystal elastomer swims into the dark. *Nat. Mater.*, 3:307–310, 2004.

[9] Y. L. Yu, M. Nakano, and T. Ikeda. Directed bending of polymer film by light – miniaturizing a simple photomechanical system could expand its range of applications. *Nature*, 425(6954):145, 2003.

[10] M. D. Kempe, N. R. Scruggs, R. Verduzco, J. Lal, and J. A. Kornfield. Self-assembled liquid-crystalline gels designed from the bottom up. *Nat. Mater.*, 3(3):177–182, 2004.

[11] M. D. Kempe, R Verduzco, N. R. Scruggs, and J. A. Kornfield. Rheological study of structural transitions in triblock copolymers in a liquid crystal solvent. *Soft Matter*, 2(5):422–431, 2006.

[12] I.-C. Khoo and S.-T. Wu. *Optics and Nonlinear Optics of Liquid Crystals.* World Scientific, Singapore, 1993.

[13] M. Warner and E.M. Terentjev. Nematic elastomers – a new state of matter? *Prog. Polym. Sci.*, 21:853–891, 1996.

[14] Pierre-Gilles de Gennes. *The Physics of Liquid Crystals.* Clarendon Press, Oxford, 2nd edition, 1993.

[15] K. Skarp, S. T. Lagerwall, and B. Stebler. Measurements of hydrodynamic parameters for nematic 5cb. *Mol. Cryst. Liq. Cryst.*, 60:215–236, 1980.

[16] E. M. Terentjev, M. Warner, R. B. Meyer, and J. Yamamoto. Electromechanical fredericks effects in nematic gels. *Phys. Rev. E*, 60(2):1872–1879, 1999.

[17] O. D. Lavrentovich and V. M. Pergamenshchik. Stripe domain phase of a thin nematic film and the k_{13} divergence term. *Phys. Rev. Lett.*, 74(7):979–982, 1994.

[18] V. M. Pergamenshchik. Spontaneous deformations of the uniform director ground state induced by the surfacelike elastic terms in a thin planar nematic layer. *Phys. Rev. E*, 61(4):3936–3941, 2000.

[19] G. C. Verwey, M. Warner, and E. M. Terentjev. Elastic instability and stripe domains in liquid crystalline elastomers. *J. Phys. II*, 6:1273–1290, 1996.

[20] C. C. Chang, L. C. Chien, and R. B. Meyer. Electro-optical study of nematic elastomer gels. *Phys. Rev. E*, 56(1):595–599, 1997.

[21] M. A. Grinfeld. The stress driven instability in elastic crystals: mathematic models and physical manifestations. *J. Nonlinear Sci.*, 3:35–83, 1993.